NANO LETTERS

2006
Vol. 6, No. 11
2472−2477

Organic Light-Emitting Diodes Having Carbon Nanotube Anodes

Jianfeng Li,[†] Liangbing Hu,[‡] Lian Wang,[†] Yangxin Zhou,[‡] George Grüner,*[,‡] and Tobin J. Marks*[,†]

Department of Chemistry, Northwestern University, Evanston, Illinois 60208-3113, and Department of Physics, University of California, Los Angeles, California 90095

Received January 20, 2006; Revised Manuscript Received July 13, 2006

ABSTRACT

Single-walled carbon nanotube (SWNT) films on flexible PET (polyethyleneterephthalate) substrates are used as transparent, flexible anodes for organic light-emitting diodes (OLEDs). For polymer-based OLEDs having the structure: SWNT/PEDOT−PSS:MeOH/TFB (poly(9,9-dioctylfluorene-*co*-*N*-(4-butylphenyl)diphenylamine)) + TPD−Si_2 (4,4′-bis[(*p*-trichlorosilylpropylphenyl)phenylamino]biphenyl) /BT (poly(9,9-dioctylfluorene-*co*-benzothiadiazole))/CsF/Al, a maximum light output of 3500 cd/m^2 and a current efficiency of 1.6 cd/A have been achieved. The device operational lifetime is comparable to that of devices with Sn-doped In_2O_3 (ITO)/PET anodes. The advantages of this novel type of anode over conventional ITO are discussed.

The exceptional electrical and mechanical properties of single-wall carbon nanotubes (SWNTs) have now been firmly established through extensive experiments[1−6] performed on individual SWNTs. Nevertheless, key manufacturability and system integration challenges must be surmounted before full exploitation of the unique SWNT attributes is possible. A two-dimensional random network of such SWNTs is one obvious—and perhaps the most straightforward—avenue whereby statistical averaging leads to highly reproducible networks that can be fabricated at precisely tuned NT densities. For this reason, SWNT thin films cast from aqueous solutions containing various surfactants have attracted much recent attention.[7−13] These networks are transparent and highly conducting with excellent mechanical properties. Hence, there is growing interest in SWNT thin films for applications in the area of macroelectronics and optoelectronics where flexible, transparent, and conductive coatings together with simple and cheap room-temperature fabrication are required. To date, several types of devices based on thin SWNT films such as flexible transparent transistors,[14−17] optical modulators,[10] LEDs with SWNT films as p-type ohmic contacts,[18] and flexible emitter arrays[19] have been fabricated.

Theoretical and experimental studies have also established the work function of SWNT networks to be in the 4.7−5.2 eV range.[20,21] Such high work functions meet the requirement for anodes in several types of photonic devices, such as organic light-emitting diodes and organic solar cells. These characteristics and the simple room-temperature fabrication avenue, together with other attributes such as excellent mechanical flexibility, indicate that this type of novel anode is a promising candidate material for next-generation photonic device applications.

Polymer and small molecule-based organic light-emitting diodes (OLEDs) are rapidly approaching large-scale commercialization, driven by attractions such as low cost, fast response, applications in large-area flexible displays, and propelled by advances in efficiencies and operational lifetimes.[22−25] OLEDs are "dual-injection" devices in which holes and electrons are injected from the anode and cathode, respectively, into an active molecular/macromolecular medium to produce, via exciton decay, light emission.[24] Although tin-doped indium oxide (ITO) is used in numerous opto-electronic applications, it has significant limitations for current and future generation OLEDs. Diffusion of oxygen into proximate organic charge transporting/emissive layers,[26,27] significant absorption in the blue region,[28] a relatively low work function (∼4.7 eV),[29] and corrosion susceptibility[29] are just a few of the limitations. Note also that In is in relatively short supply and therefore expensive, presenting significant challenges for large-scale introduction of next-generation display and photovoltaic technologies.[30]

In this paper, we describe the fabrication of flexible polymer-based OLEDs using SWNT films as anodes. We examine the response characteristics and report that for polymer-based OLEDs, the luminous performance is close

* Corresponding authors. E-mail: (T.J.M.) t-marks@northwestern.edu; (G.G.) ggruner@ucla.edu.
[†] Department of Chemistry, Northwestern University.
[‡] Department of Physics, University of California, Los Angeles.

10.1021/nl061616a CCC: $33.50
Published on Web 10/03/2006

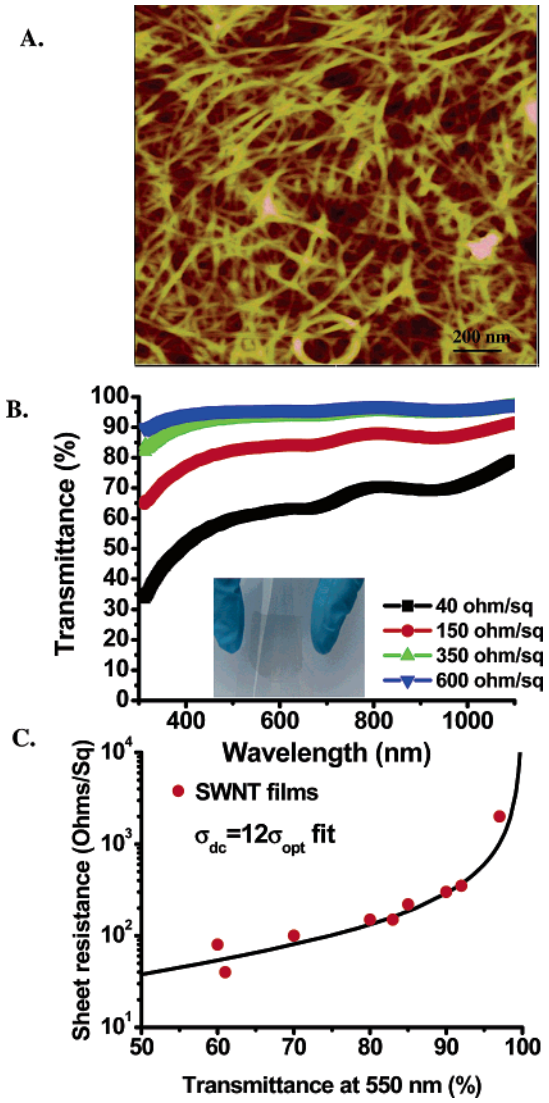

Figure 1. (A) AFM image of a transferred SWNT film on a PET substrate, showing the high pore density. The rms roughness is 6-10 nm from the AFM image. From AFMs of monolayer SWNT films, the average diameter of each bundle is ~ 4-6 nm. (B) Transmittance vs wavelength in the visible and near-infrared regions for SWNT films. The inset shows a photograph of a transferred SWNT film on a flexible PET substrate with 120 Ω/□ sheet resistance. (C) DC sheet resistance vs transmittance of SWNT films at 550 nm for various NT densities; the line shows the fit to eq 1 with $\sigma_{dc} = 12\sigma_{op}$, giving $\sigma_{dc} = 2400$ S/cm.

to that required for applications such as home television. Recently, a polymer-based OLED using an oriented *multi-walled* nanotube film anode on glass or polymer substrates was reported. The performance is well below what we report here.[31]

The process for fabricating transparent, conducting single-walled carbon nanotube films on PET substrates by filtration and transfer printing has been described previously.[32] SWNT powders purchased from Carbon Solutions Inc. are suspended in water with the surfactant SDS, followed by sonication and filtering. Washing with deionized water removes the SDS. A PDMS-based method[32] is then applied to transfer the nanotube films onto PET substrates. Figure 1A shows an AFM image of a transferred SWNT film on PET. The films have highly nanoporous structures, with specific surface areas as large as 1500 m^2/g. The rms roughness is 6−10 nm.

Transmittance measurements in the visible and infrared were carried out with a Beckman Coulter DU 640 spectrophotometer. Transmittance is only weakly dependent on the wavelength (Figure 1B), in accord with the neutral color of the film. For SWNT sheets having different thicknesses, sheet resistance and transmittance are related by eq 1:[11]

$$T = \left(1 + \frac{1}{2R_s}\sqrt{\frac{\mu_0\sigma_{op}}{\epsilon_0\sigma_{dc}}}\right)^{-2} = \left(1 + \frac{188(\Omega)}{R_s}\frac{\sigma_{op}}{\sigma_{dc}}\right)^{-2} \quad (1)$$

where the sheet resistance $R_s = 1/\sigma_{dc}t$, t is the film thickness, and the optical conductivity $\sigma_{op} = 200$ S/cm.[33] It has been shown that the optical conductivity in the visible depends only on the overall network density, while dc conductivity—and thus the measured sheet resistance—is strongly dependent on factors such as nanotube−nanotube connectivity, tube length, etc. The sheet resistance and transmittance of films at 550 nm having varying thickness (Figure 1C) are described well by eq 1, leading to $\sigma_{dc} = 2400$ S/cm by using $\sigma_{op} = 200$ S/cm.

For polymer-based OLED fabrication, a polymer blend hole-transporting layer (HTL) composed of a cross-linkable, hole-transporting organosiloxane material such as TPD−Si_2[34] and a hole-transporting polymer such as TFB (Figure 2), which also serves as an effective PLED electron-blocking layer (EBL),[35,36] was spin-coated onto a clean carbon SWNT film or onto a PEDOT−PSS-coated carbon SWNT film to form a double-layer HTL. These HTL films were then dried in a vacuum oven at 90 °C for 1−2 h. PEDOT−PSS (Baytron P) was spin-coated onto the SWNT film at 2500 rpm for 1 min, followed by drying at 120 °C for 8 min. Alternatively, a mixture of PEDOT−PSS and methanol (Baytron P:MeOH = 1:2)[37] was spin-coated onto the SWNT film at 600 rpm for 1 min, then at 2500 rpm for 1 min, followed by drying at 120 °C for 2 h in a vacuum oven. Next, a well-balanced charge transport/emissive layer (EML), a TFB + BT blend (TFB:BT = 1:4), or a electron-dominated EML, BT, was spin-coated onto the HTL-coated substrates from xylene solution, resulting in an EML thickness of ~70 nm.[35] The resulting films were then dried in a vacuum oven at ~90 °C overnight. Inside an inert-atmosphere glove box, CsF and Al were thermally evaporated onto the EML at $<10^{-6}$ Torr using a shadow mask to define the 2 mm × 5 mm electrode areas. The resulting PLEDs were characterized inside a sealed aluminum sample container under a dry N_2 atmosphere using a computer-controlled Keithley 2400 source meter and an IL 1700 Research Radiometer equipped with a calibrated photodetector.[35,36] PLED lifetime measurements were carried out using a computer-controlled Keithley 2400 source meter and an IL1400A International Light Radiometer/Photometer inside a sample container continuously purged with N_2 gas at room temperature.

The four PLED device multilayer structures characterized in this work were: SWNT/TFB + TPD−Si_2/TFB + BT/CsF/Al (device 1), SWNT/PEDOT−PSS/TFB + TPD−Si_2/

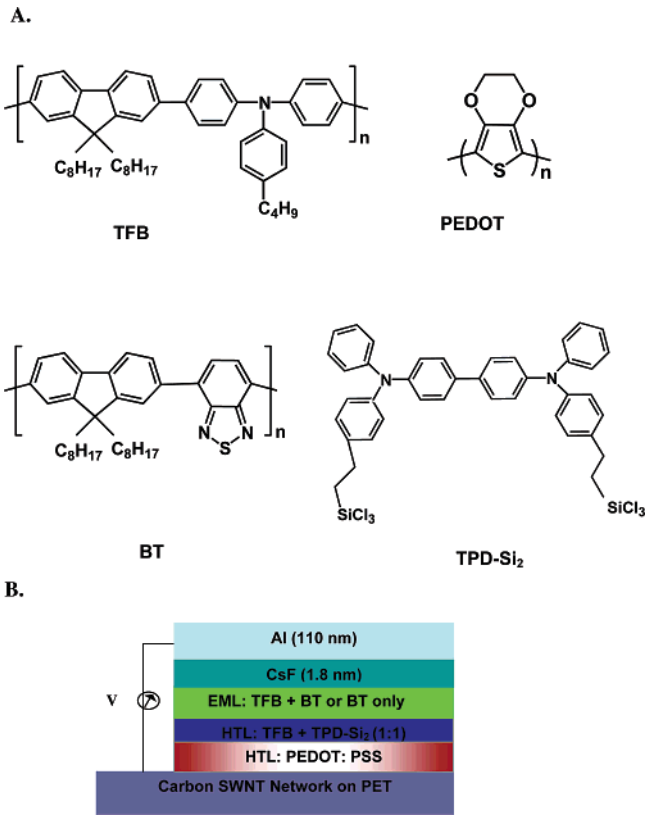

Figure 2. (A) Chemical structures of poly(9,9-dioctyl-fluorene-*co*-*N*-(4-butylphenyl)diphenylamine) (TFB), poly(9,9-dioctylfluorene-*co*-benzothiadiazole) (BT), poly(3,4-ethylenedioxythiophene) (PEDOT), and 4,4′-bis[(*p*-trichlorosilylpropylphenyl)phenylamino]-biphenyl (TPD−Si_2). (B) Structure of a PLED device having a carbon SWNT film anode.

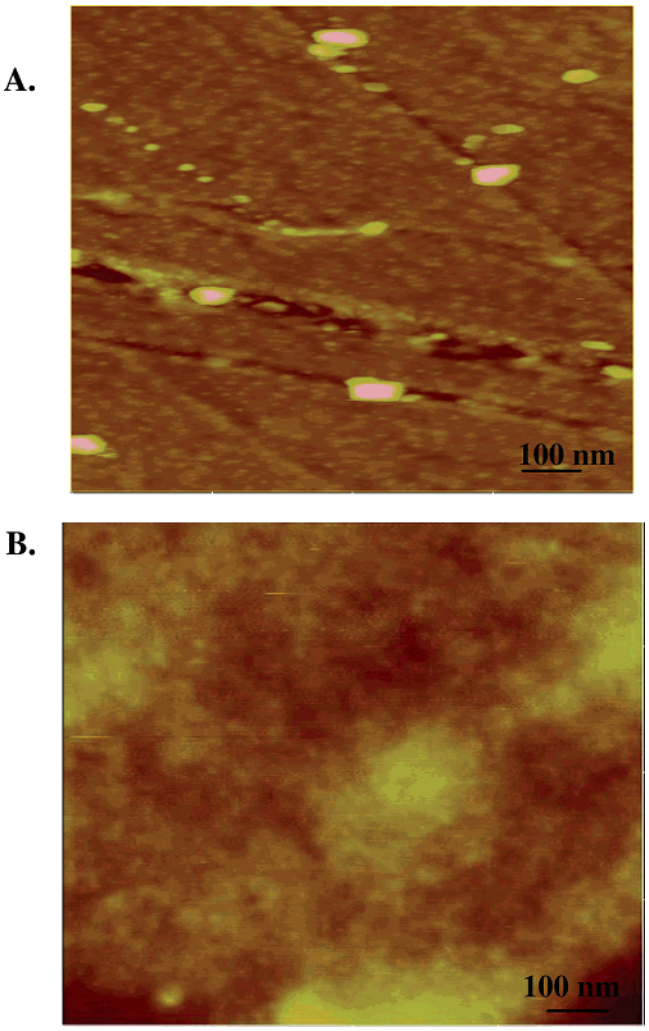

Figure 3. (A) AFM image of SWNT film with a spin-coated PEDOT−PSS overlayer. The rms roughness is 4 nm from the AFM image. (B) AFM image of SWNT film with a spin-coated PEDOT−PSS:MeOH (1:2) overlayer. The rms roughness is 0.96 nm from the AFM image.

TFB + BT/CsF/Al (device 2), SWNT/PEDOT−PSS:MeOH/TFB + TPD−Si_2/TFB + BT/CsF/Al (device 3), and SWNT/PEDOT−PSS:MeOH/TFB + TPD−Si_2/BT/CsF/Al (device 4). The current density, luminance, and current efficiency vs bias responses for these four device structures are compared in Figures 4 and 5. The PLED with PEDOT−PSS:MeOH and TFB + TPD−Si_2 as a double-layer HTL (device 3) exhibits a low turn-on voltage of 5.0 V, a maximum luminance of 1000 cd/m^2, and a maximum current efficiency of 0.85 cd/A − a greater than 3-fold increase in maximum luminance, a ∼50% lower turn-on voltage, and much greater current efficiency than the device having TFB + TPD−Si_2 only as the HTL (device 1). This may reflect the tendency of PEDOT−PSS to planarize the SWNT films while acting as a hole-transporting and buffer layer, decreasing the hole-injection barrier from the SWNTs (the PEDOT−PSS work function straddles that of SWNTs and TFB−TPD−Si_2) and minimizing device leakage currents. Furthermore, device 3 exhibits a 2-fold increase of maximum luminance and current efficiency compared with the device having spin-coated PEDOT−PSS only (device 2). This may reflect the greater tendency of PEDOT−PSS + MeOH to planarize and wet the SWNT films. The rms roughness of the SWNT film spin-coated with PEDOT−PSS:MeOH is 0.96 nm by AFM (Figure 3)—significantly smoother than that of the SWNT film spin-coated with PEDOT−PSS only (4 nm).

For the SWNT/TFB + $TPDSi_2$/TFB + BT/CsF/Al structures, rectification in the $J-V$ curve is clearly observed, with a maximum luminance of 10 cd/m^2 and a turn-on voltage of 12 V. In contrast, SWNT/PEDOT−PSS:MeOH/TFB + $TPDSi_2$/TFB + BT/CsF/Al devices with spin-coated PEDOT−PSS as the hole injection layer exhibit orders of magnitude improvements in these parameters. The maximum luminance is 1000 cd/m^2, the turn-on voltage is ∼ 5.0 V, and the maximum current efficiency is ∼ 0.85 cd/A. This dramatic enhancement in device metrics with PEDOT−PSS incorporation is likely due to several factors. First, PEDOT−PSS better wets the SWNT films than does TFB−$TPDSi_2$. Second, PEDOT−PSS:MeOH better planarizes the SWNT films. Finally, PEDOT−PSS, as hole transport layer, straddles the work functions of the SWNT films and TFB−$TPDSi_2$, thus facilitating hole injection.

In addition, as shown in Figure 5, the performance of PLED device 4 based on an electron-dominated EML (BT)

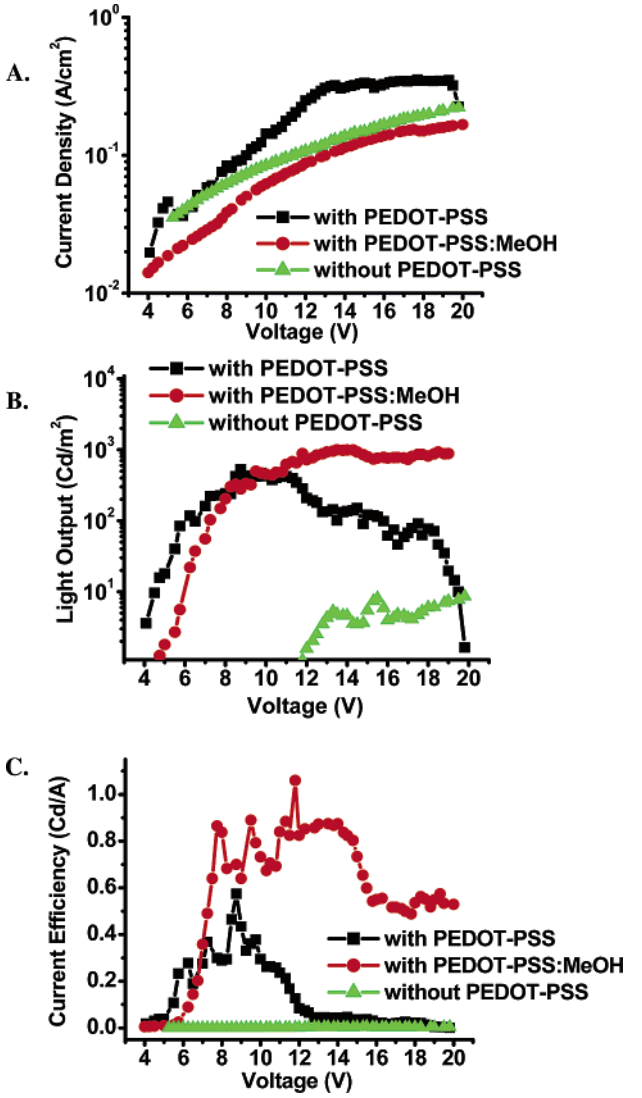

Figure 4. Response characteristics of PLEDs having the structures: (device 1) SWNT(30 nm)/PEDOT−PSS:MeOH(30 nm)/TFB + $TPDSi_2$(25 nm)/TFB + BT(70 nm)/CsF(1.8 nm)/Al(110 nm), (device 2) SWNT(30 nm)/PEDOT−PSS(30 nm)/TFB + $TPDSi_2$ (25 nm)/TFB + BT(70 nm)/CsF(1.8 nm)/Al(110 nm), and (device 3) SWNT(30 nm)/TFB + $TPDSi_2$ (25 nm)/TFB + BT (70 nm)/CsF (1.8 nm)/Al(110 nm). Key: (A) current density vs voltage; (B) luminance vs voltage; (C) current efficiency vs voltage.

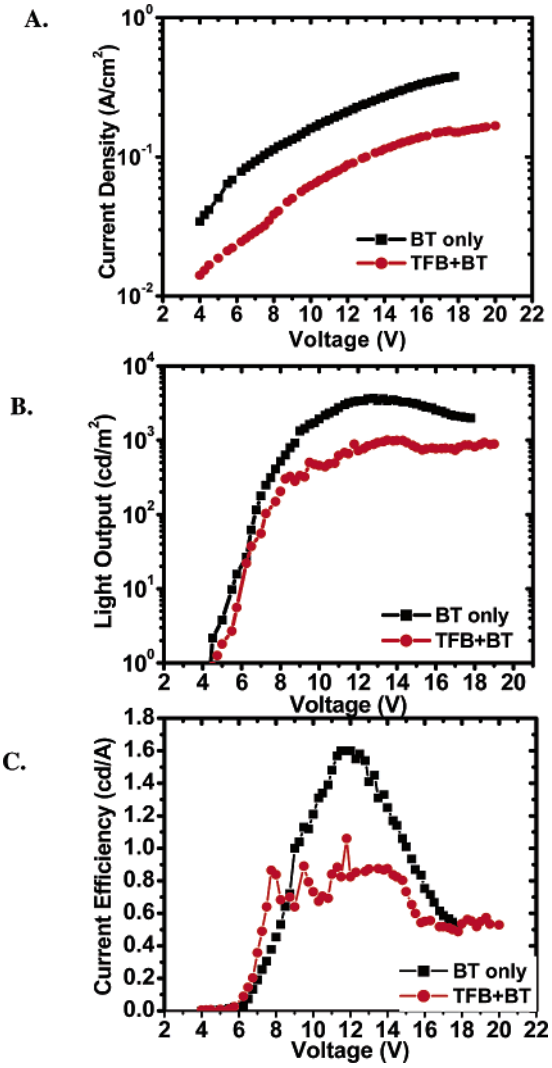

Figure 5. Response characteristics of PLEDs having the structures: (Device 3) SWNT(30 nm)/TFB + $TPDSi_2$ (25 nm)/TFB + BT (70 nm)/CsF (1.8 nm)/Al(110 nm) and SWNT(30 nm)/TFB + $TPDSi_2$ (25 nm)/ BT (70 nm)/CsF (1.8 nm)/Al(110 nm). Key: (A) current density vs voltage; (B) luminance vs voltage; (C) current efficiency vs voltage.

and an electron-blocking HTL (the TPD−Si_2 + TFB + PEDOT−PSS double layer) affords a maximum luminance = 3500 cd/m^2, and a maximum current efficiency = 1.6 cd/A, surpassing that of PLED device 3 based on a TFB + BT blend EML (TFB + BT blends are known to exhibit better balanced electron−hole transport than the BT-only EMLs). This result can be understood as follows. First, better balanced electron and hole fluences may be obtained in these PLED devices with BT-only EMLs. SWNT anode films have large surface areas, resulting in greatly enhanced hole injection.[37] Hence, greater electron−hole recombination density at the HTL/EML interface in the BT-based devices vs the TFB + BT-based devices should yield greater current efficiency and luminance. It will be seen below that longer device lifetimes are also achieved in the charge-balanced PLED device with the BT-only EML, consistent with more efficient electron−hole recombination. Furthermore, the peak recombination zone of the TFB + BT-based device should be located near the middle of the TFB + BT EML, and the relatively short distance between the peak recombination zone and the Al cathode may lead to cathode−induced exciton quenching. For the BT-based device, however, the peak recombination zone should be located nearer the TPD−Si_2 + TFB/BT interface, leading to less cathode-induced exciton quenching.

The light output of 3500 cd/m^2 achieved by the present SWNT-based PLED easily meets the requirements for many display applications, where light intensities of 100−300 cd/m^2 are required.[38] Although the present device metrics (luminance and current efficiency) do not match those found for devices using ITO anodes in similar structures,[36] the low turn-on voltage and brightness achieved are encouraging, especially taken together with the three-dimensional nature of hole injection and the SWNT film mechanical flexibility.

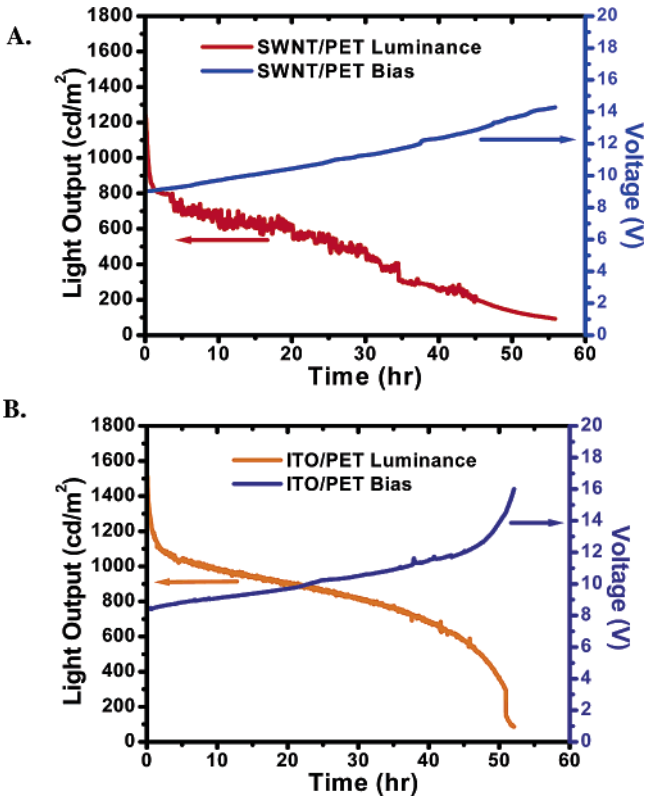

Figure 6. Life time characterization of PLEDs having the structures: (A) SWNT on PET/PEDOT−PSS:MeOH(30 nm)/TFB + $TPDSi_2$(25 nm)/BT(70 nm)/CsF(1.8 nm)/Al(110 nm) and (B) ITO on PET/PEDOT−PSS:MeOH(30 nm)/TFB + $TPDSi_2$(25 nm)/BT(70 nm)/CsF(1.8 nm)/Al(110 nm).

We also evaluated the lifetimes of the SWNT-based PLEDs. The operational lifetime of device 4 was obtained under DC (continuously ON) conditions with a 0.12 A/cm^2 constant current density at room temperature, under a dry N_2 purge. The lifetime was found to be ∼ 55 h with 1200 cd/m^2 initial luminance (L_0; Figure 6 A). For comparison, an ITO/PET-(purchased from CP Films Inc., sheet resistance = 200 Ω/□, ∼ 3 nm rms roughness) based PLED device having the same configuration as device 4 was fabricated in parallel. The ITO/PET-based control device, which has a maximum light output of 20,000 cd/m^2 and a maximum current efficiency of 6 cd/m^2, exhibits a comparable operational lifetime of ∼ 52 h with L_0 = 1400 cd/m^2 (Figure 6B) under identical measurement conditions. Note that all lifetime data were obtained from unencapsulated devices.

Although the output parameters of the present SWNT-based PLEDs are modest at this stage compared to ITO-based PLEDs,[36] our results suggest potential as ITO alternatives for several reasons. (1) SWNT films on PET exhibit sheet resistances of 120 Ω/□ with 80% transmittance, metrics comparable to commercial ITO on plastic. By doping SWNT films with NO_2, a 3-fold decrease in sheet resistance without change of transparency can be expected.[39] (2) The exceptional mechanical flexibility of SWNT films has been demonstrated.[15,16] In contrast, ITO films on plastic crack after repeated bending. As shown by Sarran et al.[12] and also by us, SWNT films on PET do not crack or crease after bending, while ITO films become insulating. (3) SWNT films on PET exhibit good acid resistance, while ITO is quickly corroded, even by PEDOT−PSS solutions.[22,29] (4) Due to excellent surface energy matching, SWNT films adhere strongly to PET and PMMA, passing the "Scotch tape" decohesion test. (5) SWNT films, due to the nanoporous structure, have surface areas as great as 1500 m^2/g, offering hole injection potential. (6) SWNT film fabrication on PET, starting from SWNT powders, is a room-temperature process and relatively simple, while ITO deposition on flexible substrates requires vacuum and elaborate process equipment. Room-temperature processing renders the SWNT films suitable for use with a wide range of substrates for both top and bottom emission devices.

Acknowledgment. We thank the NASA Institute for Nanoelectronics and Computing (NCC2-3163) for support of this research. Characterization facilities were provided by the Northwestern University MRSEC program (NSF-DMR-00760097). Research at UCLA was supported by NSF Grant DMR-0404029. We also thank Mr. P. Russell for writing the lifetime data analysis software and Mr. M. Russell for the helpful discussions.

Note Added after ASAP Publication. The manuscript received date was incorrect in the version published ASAP on October 3, 2006; the corrected version was published ASAP October 5, 2006.

References

(1) Tans, S. J.; Verschueren, A. R. M.; Cees, D. *Nature* **1998**, *393*, 49.
(2) Stadermann, M.; Papadakis, S. J.; Falvo, M. R.; Novak, J.; Snow, E.; Fu, Q.; Liu, J.; Fridan, Y.; Boland, J. J.; Superfine, R.; Washburn, S. *Phys. Rev. B* **2004**, *69*, 201402/1.
(3) Durkop, T.; Getty, S. A.; Cobas, E.; Fuhrer, M. S. *Nano. Lett.* **2004**, *4*, 35.
(4) Perebeinos, V.; Tersoff, J.; Avouris, P. *Phys. Rev. Lett.* **2005**, *94*, 027402/1.
(5) Stahl, H.; Appenzeller, J.; Martel, R.; Avouris, P.; Lengeler, B. *Phys. Rev. Lett.* **2000**, *85*, 5186.
(6) Zhou, C.; Kong, J.; Dai, H. *Phys. Rev. Lett.* **2000**, *84*, 5604.
(7) Moore, V. C.; Strano, M. S.; Haroz, E. H.; Hauge, R. H.; Smalley, R. E.; Schmidt, J.; Talmon, Y. *Nano. Lett.* **2003**, *3*, 1379.
(8) Bekyarova, E.; Itkis, M. E.; Cabrera, N.; Zhao, B.; Yu, A.; Gao, J.; Haddon, R. C. *J. Am. Chem. Soc.* **2005**, *127*, 5990.
(9) Kaempgen, M.; Duesberg, G. S.; Roth, S. *Appl. Surf. Sci.* **2005**, *252*, 425.
(10) Wu, Z.; Chen, Z.; Du, X.; Logan, J. M.; Sippel, J.;Nikolou, M.; Kamaras, K.; Reynolds, J. R.; Tanner, D. B.; Hebard, A. F.; Rinzler A. G. *Science* **2004**, *305*, 1273.
(11) Hu, L.; Hecht, D. S.; Grüner, G. *Nano Lett.* **2004**, *4*, 2513.
(12) Saran, N.; Parikh, K.; Suh, D.-S.; Munoz, E.; Kolla, H.; Manohar, S. K. *J. Am. Chem. Soc.* **2004**, *126*, 4462.
(13) Hur, S.-H.; Park, O. O.; Rogers, J. A. *Appl. Phys. Lett.* **2005**, *86*, 243502.
(14) Bradley, K.; Gabriel, J.−C. P.; Grüner, G. *Nano Lett.* **2003**, *3*, 1353.
(15) Artukovic, E.; Kaempgen, M.; Hecht, D. S.; Roth, S.; Grüner, G. *Nano Lett.* **2005**, *5*, 757.
(16) Snow, E. S.; Campbell, P. M.; Ancona, M. G.; Novak, J. P. *Appl. Phys. Lett.* **2005**, *86*, 033105/1.
(17) Cao, Q.; Hur, S.−H., Zhu, Z.−T.; Sun, Y. G.; Wang, C.−J.; Meitl, M. A.; Shim, A.; Rogers, J. A. *Adv. Mater.* **2006**, *18*, 304.
(18) Lee, K.; Wu, Z.; Chen, Z.; Ren, F.; Pearton, S. J.; Rinzler, A. G. *Nano Lett.* **2004**, *4*, 911.
(19) Yoon, B.−J.; Hong, E. H.; Jee, S. E.; Yoon, D.−M.; Shim, D.−S.; Son, G.−Y.; Lee, Y. J.; Lee, K.−H.; Kim, H. S.; Park, C. G. *J. Am. Chem. Soc.* **2005**, *17*, 4049.
(20) Suzuki, S.; Bower, C.; Watanabe, Y.; Zhou, O. *Appl. Phys. Lett.* **2000**, *76*, 4007.
(21) Zhao, J.; Han, J.; Lu, J. P. *Phys. Rev. B*, **2002**, *65*, 193401/1.

(22) Veinot, J. G. C.; Marks, T. J. *Acc. Chem. Res*., **2005**, *38*, 632.
(23) Chen, C.−T. *Chem. Mater.* **2004**, *16*, 4389.
(24) Mitschke, U.; Bauerle, P. *J. Mater. Chem.* **2000**, *10*, 1471.
(25) Shim, H.−K.; Jin, J.−I. *Adv. Polym. Sci.* **2002**, *158*, 193.
(26) Schlatmann, A. R.; Floet, D. W.; Hillberer, A.; Garten, F.; Smulders, P. J. M.; Klapwijk, T. M.; Hadziioannou, G. *Appl. Phys. Lett*. **1996**, *69*, 1764.
(27) Scott, J. C.; Kaufman, J. H.; Brock, P. J.; Dipietro, R.; Salem, J.; Goitia, J. A. *J. Appyl. Phys.* **1996**, *79*, 2745.
(28) Philips, J. M.; Kwo, J.; Thomas, G. A.; Carter, S. A.; Cava, R. J.; Hou, S. Y.; Krajewski, J. J.; Marshall, J. H.; Peck, W. F.; Rapkine, D. H.; Dover, R. B. V. *Appl. Phys. Lett.* **1994**, *65*, 115.
(29) Ni, J.; Yan, H.; Wang, A.; Yang, Y.; Stern, C. L.; Metz, A. W.; Jin, S.; Wang, L.; Marks, T. J.; Ireland, J. R.; Kannewurf. C. R. *J. Am. Chem. Soc.* **2005**, *127*, 5613.
(30) Jansseune, T. *Compd. Semiconductor Mag.* **2003**, Sept.
(31) Zhang, M.; Fang, S.; Zakhidov, A., A.; Lee, S. B.; Aliev, A. E.; Williams, C. D.; Atkinson, K. R.; Baughman, R. H. *Science*, **2005**, *309*, 1215.
(32) Zhou, Y.; Hu, L.; Grüner, G. *Appl. Phys. Lett.* **2006**, *88*, 1231091
(33) Ruzicka, B.; Degiorgi, L.; Gaal, R.; Thien-Nga, L.; Bacsa, R.; Salvetat, J.P.; Forro, L. *Phys. Rev. B* **2000**, *61*, 2468.
(34) Huang, Q.; Evmenenko, G. A.; Dutta, P.; Lee, P.; Armstrong, N. R.; Marks, T.J. *J. Am. Chem. Soc.* **2005**, *127*, 10227.
(35) Yan, H.; Scott, B.; Huang, Q.; Marks, T. J. *Adv. Mater.* **2004**, *16*, 1948.
(36) Yan, H.; Lee, P.; Armstrong, N. R.; Graham, A.; Evmenenko, G. A.; Dutta, P.; Marks, T. J. *J. Am. Chem. Soc.* **2005**, *127*, 3172.
(37) Pasquier, A. D.; Unalan, H. E.; Kanwal, S. M.; Chhowalla, M. *Appl. Phys. Lett.* **2005**, *87*, 203511.
(38) *Organic light-emitting materials and device VII*; Kafafi, Z. H., Lane, P. A., Eds.; Proceedings of SPIE 5214 SPIE: Bellingham, WA, 2003; p 40.
(39) Hecht, D; Gruner, G. Unpublished work.

NL061616A